applied microbiology

MDPI

Article

Living in a Puddle of Mud: Isolation and Characterization of Two Novel *Caulobacteraceae* Strains *Brevundimonas pondensis* sp. nov. and *Brevundimonas goettingensis* sp. nov.

Ines Friedrich [1], Anna Klassen [1], Hannes Neubauer [1], Dominik Schneider [1], Robert Hertel [2] and Rolf Daniel [1,*]

[1] Genomic and Applied Microbiology and Göttingen Genomics Laboratory, Institute of Microbiology and Genetics, Georg-August-University of Göttingen, 37077 Göttingen, Germany; ines.friedrich@uni-goettingen.de (I.F.); ge35ruh@mytum.de (A.K.); hannes.neubauer@stud.uni-goettingen.de (H.N.); dschnei1@gwdg.de (D.S.)

[2] FG Synthetic Microbiology, Institute of Biotechnology, BTU Cottbus-Senftenberg, 01968 Senftenberg, Germany; hertel@b-tu.de

* Correspondence: rdaniel@gwdg.de

Abstract: *Brevundimonas* is a genus of freshwater bacteria belonging to the family *Caulobacteraceae*. The present study describes two novel species of the genus *Brevundimonas* (LVF1^T and LVF2^T). Both were genomically, morphologically, and physiologically characterized. Average nucleotide identity analysis revealed both are unique among known *Brevundimonas* strains. In silico and additional ProphageSeq analyses resulted in two prophages in the LVF1^T genome and a remnant prophage in the LVF2^T genome. Bacterial LVF1^T cells form an elliptical morphotype, in average 1 µm in length and 0.46 µm in width, with a single flagellum. LVF2^T revealed motile cells approximately 1.6 µm in length and 0.6 µm in width with a single flagellum, and sessile cell types 1.3 µm in length and 0.6 µm in width. Both are Gram-negative, aerobic, have optimal growth at 30 °C (up to 0.5 to 1% NaCl). Both are resistant towards erythromycin, meropenem, streptomycin, tetracycline and vancomycin. Anaerobic growth was observed after 14 days for LVF1^T only. For LVF1^T the name *Brevundimonas pondensis* sp. nov. and for LVF2^T the name *Brevundimonas goettingensis* sp. nov. are proposed. Type strains are LVF1^T (=DSM 112304^T = CCUG 74982^T = LMG 32096^T) and LVF2^T (=DSM 112305^T = CCUG 74983^T = LMG 32097^T).

Keywords: *Brevundimonas*; phage host system; prophages; *Caulobacteraceae*

Citation: Friedrich, I.; Klassen, A.; Neubauer, H.; Schneider, D.; Hertel, R.; Daniel, R. Living in a Puddle of Mud: Isolation and Characterization of Two Novel *Caulobacteraceae* Strains *Brevundimonas pondensis* sp. nov. and *Brevundimonas goettingensis* sp. nov.. *Appl. Microbiol.* **2021**, *1*, 38–59. https://doi.org/10.3390/applmicrobiol1010005

Academic Editor: Zuzanna Drulis-Kawa

Received: 6 April 2021
Accepted: 11 May 2021
Published: 13 May 2021

1. Introduction

The bacterial family *Caulobacteraceae* belongs to the α-subclass of Proteobacteria and is the only member within the order Caulobacterales [1]. It includes the genera *Asticcacaulis*, *Brevundimonas*, *Caulobacter* and *Phenylobacterium* [2]. The members of *Caulobacteraceae* thrive in diverse habitats such as freshwater, seawater, soil, plants and humans [3]. All members are Gram-negative, aerobic or facultative anaerobic, and rod-shaped or vibrioid. They divide asymmetrically while one cell is sessile with prosthecae [4], and the other cell is motile with a polar flagellum [5]. The swarmer daughter cells move freely in the environment until they form a stalk and attach to substrates [6]. The stalked cell has the ability to divide asymmetrically. This unusual cell cycle was intensively studied in *Caulobacter*. Representatives of the genus *Caulobacter* often occur in "rosettes", which can be interpreted as clusters of stalk cells attached to each other in groups [7]. The single-celled organism was originally described in 1935 by Henrici and Johnson based on microscopic findings with respect to microorganisms attached to microscopic slides that had been hatched in a freshwater lake (Henrici and Johnson, 1935).

Caulobacter has a broad habitat range and occurs in freshwater, seawater and terrestrial environments [8]. Their closest relatives are organisms that are classified as members of the

genus *Brevundimonas* [9]. The genus *Brevundimonas* was introduced based on the reclassification of two *Pseudomonas* species as *Brevundimonas diminuta* and *Brevundimonas vesicularis* [9]. *Brevundimonas* appears in various habitats such as soils, deep subseafloor sediments, activated sludge, black sand, blood, and aquatic habitats [10–16]. They are usually non-prosthecate motile bacteria with polar flagella with only a few sessile species [11,16–18]. Abraham et al., suggest that species from the genus *Brevundimonas* may have lost the ability to form prosthecate during evolution or permanently migrated in the motile stage of the developmental cycle [2].

Moreover, *Brevundimonas* and *Caulobacter* are similar regarding their lifestyles. Both species are K-strategists and can survive under oligotrophic conditions [19]. There are no nutritional characteristics that distinguish both genera clearly. Therefore, *Caulobacter* strains such as *Caulobacter subvibrioides*, *Caulobacter bacteroides* and *Caulobacter vesicularis* were reclassified to *Brevundimonas subvibrioides*, *Brevundimonas bacteroides* and *Brevundimonas vesicularis*, respectively [2]. Nowadays, 32 *Brevundimonas* species and 12 *Caulobacter* species (LPSN [20] accessed on 1 November 2020) are known.

Three phages infecting *Asticcacaulis biprosthecium* are known [3] and seven *Brevundimonas vesicularis*-associated phages have been isolated and genetically characterized [21]. *Caulobacter*-associated phages like *Caulobacter vibrioides* CB13B1a bacteriophage φCd1 is an icosahedral DNA phage with a short non-contractile tail. It infects both prosthecate and swarmer cells [22]. Besides common dsDNA phages [23], RNA phages are known to infect *Caulobacteraceae*, i.e., φCb5, a small polyhedral RNA phage belonging to the *Leviviridae* family. The phage has been broadly used as model for molecular biology studies [24,25]. The verified association of *Caulobacter* with diverse phage types indicates that this genus is suitable for analysis of exceptionally diverse viral communities. This contributes also to how a virome associated with a particular host is composed concerning the ssDNA, dsDNA, dsRNA and ssRNA genomes of its phages. The aim of the present investigation was to isolate and characterize a bacterial strain of the *Caulobacteracea* family suitable to serve in further studies as a host system to access the viral diversity of *Caulobacteracea*-related phages present in the environment.

2. Materials and Methods

2.1. Isolation of the Bacteria and DNA Extraction

Environmental samples of twelve different sampling sites were collected. Six samples were taken from an oligotrophic pond located in the northern part of Weende, Göttingen, Germany. These environmental samples derived from frog's lettuce (*Groenlandia densa*) (PM), pond water (PW), surface water near pond algae (WSA), surface water near frog's lettuce (WSP), surface water of reed (WSR) and surface water close from Weende River entrance (WSW). Additionally, three samples were collected from the Weende River nearby the oligotrophic pond. Those samples are river water (RW) and (mixed = different sizes) river stones (RS and MRS). Further, two samples were gathered from a eutrophic pond at the North Campus of the Georg-August University Göttingen, which are surface water (POW) and surface water of stale eutrophic pond (PSW). In addition, samples from a puddle close by the eutrophic pond were collected as well (PUW). The specific coordinates of the sites and dates of the sampling are depicted in Table 1.

Table 1. Coordinates of sampling sites and dates sampling.

Samples	Coordinates	Date
MRS	51°33′58″ N 9°56′18″ E 230 m	6 September 2018
PW	51°33′57″ N 9°57′20″ E 230 m	6 September 2018
RS	51°33′58″ N 9°56′18″ E 230 m	6 September 2018
RW	51°33′58″ N 9°56′18″ E 230 m	6 September 2018
WSP	51°33′59″ N 9°56′22″ E 230 m	11 September 2018
WSW	51°33′59″ N 9°56′23″ E 230 m	11 September 2018
WSA	51°33′58″ N 9°56′22″ E 230 m	11 September 2018
WSR	51°33′58″ N 9°56′22″ E 230 m	11 September 2018
PM	51°33′58″ N 9°56′22″ E 230 m	11 September 2018
POW	51°33′29″ N 9°56′41″ E 173 m	24 September 2018
PSW	51°33′29″ N 9°56′41″ E 173 m	24 September 2018
PUW	51°33′27″ N 9°56′40″ E 173 m	24 September 2018

Enrichment cultures were performed as described by Friedrich et al., (2020, 2021) and Hollensteiner et al., (2021) using environmental water samples and river stones as inoculum for peptone medium containing 0.001% (*w*/*v*) peptone (Carl Roth GmbH + Co. KG, Karlsruhe, Germany) [26–28]. Cultures were incubated undisturbed for three weeks at 25 °C [29]. Additionally, MRS, PW, RS, and RW were enriched with 5% (*v*/*v*) MeOH and 0.001% (*w*/*v*) peptone. Biofilm and water surface material were sampled and streaked on 0.05% peptone-containing agar medium supplemented with 1% vitamin solution No. 6 [4] and 1.5% agar. After colony formation, they were transferred onto a diluted peptone agar plate supplemented with $CaCl_2$ (PCa) [29] and incubated for four days at 25 °C. For the singularization, colonies were re-streaked at least four consecutive times.

Singularized colonies were cultured in liquid PCa medium. Bacterial genomic DNA was extracted with MasterPure™ complete DNA and RNA purification kit as recommended by the manufacturer (Epicentre, Madison, WI, USA). Bacterial cells were suspended in 500 µL Tissue and Cell Lysis Solution and transferred into Lysing Matrix B tubes (MP Biomedicals, Eschwege, Germany) and mechanically disrupted for 10 s at 6.5 m/s using FastPrep®-24 (MP Biomedicals, Eschwege, Germany). After centrifugation for 10 min at 11,000× *g*, the supernatant was transferred into a 2.0 mL tube and 1 µL of Proteinase K (20 mg/mL; Epicenter) was added. The procedure was performed as recommended by the manufacturer with the modification of increasing MPC Protein Precipitation Reagent to 300 µL.

2.2. Amplicon Based 16S rRNA Gene Sequencing of Enrichment Cultures

The bacterial composition of each sample was determined via amplicon-based analysis of the V3-V4 region of the 16S rRNA gene using the bacterial primers S-D-Bact-0341-b-S-17 and S-D-Bact-0785-a-A-21 [30] containing adapters for Illumina MiSeq sequencing (Illumina, San Diego, CA, USA). The PCR reaction solution (50 µL) contained 1-fold Phusion GC buffer, 200 µM dNTPs, 5% DMSO, 0.2 µM of each primer, 200 µM $MgCl_2$, 1 U Phusion polymerase (Thermo Fisher Scientific, Waltham, MA, USA) and 25 ng extracted DNA. Initial denaturation was performed at 98 °C for 1 min, followed by 25 cycles of denaturation at 98 °C for 45 s, annealing at 55 °C for 45 s and elongation at 72 °C for 45 s. The final elongation was for 5 min at 72 °C. PCR Reactions were performed in triplicate for each sample. The resulting PCR products were pooled in equal amounts and purified through MagSi-NGS^{PREP} Plus as recommended by the manufacturer (MagnaMedics, Aachen, Germany). Quantification of the PCR products was performed using the Quant-iT dsDNA HS assay kit and a Qubit fluorometer (Invitrogen, Carlsbad, CA, USA). Illumina paired-end sequencing libraries were constructed using the Nextera XT DNA sample preparation kit (Illumina, Inc., San Diego, CA, USA). Sequencing was performed with an Illumina MiSeq instrument using the dual index paired-end approach (2 × 300 bp) and V3 chemistry as recommended by the manufacturer (Illumina). The sequencing was performed in-house by the Göttingen Genomics Laboratory.

The 16S rRNA genes of specific isolates were amplified with the primer pair 27F (5′-AGAGTTTGATCMTGGCTCAG-3′) and 1492R (5′-TACGGYTACCTTGTTACGACTT-3′) [31]. PCR reaction mixture (50 µL) contained 10 µL 5-fold Phusion HF buffer, 200 µM of each dNTP, 3% DMSO, 0.2 µM of each primer, and 1 U Phusion polymerase (Thermo Fisher Scientific, Waltham, MA, USA) and 100 ng DNA. The previously mentioned cycling scheme was modified to an annealing temperature of 50 °C and 30 cycles. Sanger sequencing of the PCR products was done by Microsynth Seqlab (Göttingen, Germany).

2.3. Amplicon Sequence Analysis

Raw paired-end reads from the Illumina MiSeq were quality-filtered with fastp v0.20.0 [32]. Default settings were used with the addition of an increased per base phred score of 20, 5′- and 3′-end read-trimming with a sliding window of 4, a mean quality of 20, minimal sequence length of 50 bp and removal of paired-end read adapters. The paired-end reads were merged using PEAR v0.9.11 [33]. Potential remaining primer sequences were clipped with cutadapt v2.5 [34]. VSEARCH v2.14.1 [35] was used to sort and size-filter the merged reads using a minimum sequence length of 300 bp. Then, reads were dereplicated and denoised with UNOISE3 [36] using default settings. Finally, chimeras were removed de novo and afterwards reference-based against the SILVA SSU database v138.1 [37] resulting in the final set of amplicon sequence variants (ASVs). Quality-filtered and merged reads were mapped against the ASVs to create an abundance table with VSEARCH using default settings. The taxonomy was assigned using BLAST 2.9.0+ [38] against the SILVA SSU 138.1 NR database [37] with an identity of at least 90% to the query sequence. To improve classification results, the best hits were only accepted if "% sequence identity +% alignment coverage)/2 $\geq$ 93" (see SILVAngs_User_Guide_2019_08_29.pdf). Additionally, all extrinsic taxa (Chloroplast, Eukaryota, Mitochondria, Archaea) were removed from the dataset resulting in a total of 1029 amplicon sequence variants (ASVs). The dataset was analyzed in R (v4.0.2) [39] and RStudio (v1.3.1056) [40]. Bar charts were generated with ggplot2 (v3.3.2) [41] using standard R packages.

2.4. Genome Sequencing, Assembly and Annotation

Illumina paired-end sequencing libraries were prepared using Nextera XT DNA Sample Preparation kit and sequenced using the MiSeq-system and reagent kit version 3 (2 × 300 bp) as recommended by the manufacturer (Illumina, San Diego, CA, USA). To perform Nanopore sequencing, 1.5 µg DNA were utilized for library preparation using Ligation Sequencing kit (SQK-LSK109) and Native Barcode Expansion kit EXP-NBD103 (Barcodes 4 and 5; Oxford Nanopore Technologies, Oxford, UK). Sequencing was performed for 72 h by using MiniON device, a SpotON Flow Cell and MinKNOW software v19.05.00 as recommended by the manufacturer (Oxford Nanopore Technologies). For demultiplexing, Guppy version v3.0.3 was employed. Raw Illumina MiSeq sequences were adapter—and quality—trimmed employing Trimmomatic v0.39 [42] and paired reads joined with FLASH v1.2.11 [43]. Nanopore reads were adapter- and quality-trimmed with fastp v0.20.0 [32] and only reads >10 kb were included in further analysis. The obtained quality-filtered Nanopore reads served as input for a hybrid assembly employing the Unicycler pipeline v0.4.9b in normal mode [44], which included SPAdes v3.14.1 [45], Racon vv.1.4.15 [46], makeblastdb v2.10.0+ and tblastn v.2.10.0+ [47], bowtie2-build v2.4.1, bowtie2 v.2.4.1 [48], SAMtools v.1.10 [49], java v.1.8.0_152 [50], and Pilon v.1.23 [51]. Illumina short-read coverage information was obtained through read-mapping with bowtie2 to the final genome. Mapping and sorting was done with SAMtools and analysis with Qualimap v.2.2.2 [52]. Nanopore long-read coverage information was obtained through QualiMap v.2.2.2. Mapping, sorting and analysis were performed as described for the short reads. Genome orientation of both genomes was performed based on the gene encoding the chromosomal replication initiation protein DnaA. Assembled genomes were checked with Bandage v0.8.1 [53]. CRISPR regions were identified with CRISPRFinder [54]. Quality of assembled genomes was assessed with CheckM v1.1.2 [55] (Supplementary Table S1).

Genome annotation was performed using the Prokaryotic Genome Annotation Pipeline v4.13 (PGAP) [56].

2.5. Preparation and Sequencing of Prophages and Visualization Using TraV

An overnight culture of *Brevundimonas* sp. nov. LVF1^T and LVF2^T was set up in a 100 mL Erlenmeyer flask using 25 mL PYE medium (0.2% peptone, 0.1% yeast extract, 0.02% $MgSO_4$ x 7 H_2O) and inoculated with an OD_{600} of 0.1. The cultures were incubated over a 3-day period on a shaker (180 rpm, Infors HT (Orbitron, Einsbach, Germany)) at 30 °C without using Mitomycin C for prophage induction [57]. After the incubation period, the cultures were transferred into a 50 mL centrifuge tube and centrifuged at 10,020× *g* and 4 °C for 15 min. The supernatant was sterile-filtered (0.2 µm pore size of filter) and supplemented with PEG-8000 (10% (*w*/*v*) final concentration), $MgSO_4$ (1 mM final concentration) and 5 µL salt-active nuclease (SERVA Electrophoresis GmbH, Heidelberg, Germany). The suspension was precipitated for 24 h at 4 °C and centrifuged at 10,020× *g* and 4 °C for 1 h. The supernatant was discarded, and the pellet suspended in 300 µL TMK buffer (10 mM Tris, 5 mM $MgCl_2$, 300 mM KCl, pH 7.5).

Prophage DNA was extracted with MasterPure™ complete DNA and RNA purification kit and was sequenced using the above-mentioned protocol for Illumina genome sequencing.

Illumina MiSeq raw paired-end reads were merged and adapter and quality-trimmed employing Trimmomatic v0.39 [42]. Sequences were then mapped against the host genome through bowtie2 v2.4.1 [48]. SAM table was converted to TDS format (flat file data format), which is the input for TraV (Transcriptome Viewer). The program TraV was designed to map transcriptome data on a genome [58]. In this study, it was employed to display the read coverages from the sequencing runs for the prophages of LVF1^T and LVF2^T mapped onto their host genomes [59]. Integration sites of the prophages (*attL* and *attR* sites) were identified through the comparison of experimentally indicated *att* regions (1 kb to each side from the indicated coordinate), against the remaining genome sequence.

2.6. Phylogenetic Classification of Brevundimonas sp. nov. LVF1^T and LVF2^T

To provide an initial taxonomic classification of the *Brevundimonas* sp. nov. isolates, Genome Taxonomy Database Toolkit (GTDB-Tk) v1.0.2 [60] was employed. In addition, a phylogenetic analysis was performed with ANIm method of pyani v0.2.10 [61]. The typical percentage threshold for species boundary (95% ANI) was used [62]. Based on the list of Deutsche Sammlung von Mikroorganismen und Zellkulturen (DSMZ, Braunschweig, Germany), available type strain genomes were downloaded from the National Centre for Biotechnological Information (NCBI, accessed 30 September 2020) including *B. alba* DSM 4736^T (PRJNA583246), *B. aurantiaca* DSM 4731^T (PRJNA583252), *B. aveniformis* DSM 17977^T (PRJNA185350), *B. bacteroides* DSM 4726^T (PRJNA221004), *B. basaltis* DSM 25335^T (PRJNA632231), *B. bullata* HAMBI_262^T (PRJNA224116), *B. diminuta* NCTC 8545^T (PRJEB6403), *B. halotolerans* DSM 24448^T (PRJNA546766), *B. halotolerans* MCS24^T (PRJNA484836) *B. lenta* DSM 23960^T (PRJNA583271), *B. mediterranea* DSM 14878^T (PRJNA583270), *B. naejangsanensis* DSM 23858^T (PRJNA188849), *B. nasdae* JCM 11415^T (PRJNA269640), *B. subvibrioides* ATCC 15264^T (PRJNA36643), *B. terrae* DSM 17329^T (PRJNA546765), *B. vancanneytii* NCTC 9239^T (PRJEB6403), *B. variabilis* DSM 4737^T (PRJNA583272), *B. vesicularis* NBRC 12165^T (PRJDB1343) and *B. viscosa* CGMCC 1.10683^T (PRJEB17543). The type strain genome of the species *B. halotolerans* was sequenced twice (DSM 14878^T and MCS24^T). Both were included in the analysis due to their differences in coverage and annotation.

2.7. Comparative Genomics

Metabolic analysis of LVF1^T and LVF2^T was investigated using BlastKOALA v2.2 [63] (Supplementary Figure S1). Putative secondary metabolite biosynthetic gene clusters were identified with antiSMASH v5.2.0 [64,65]. Putative phage regions were identified with

PHASTER [66]. Antibiotic resistance annotation was investigated employing Resfams v1.2.2 [67].

2.8. Cell Morphology and Gram Staining Procedure

Colony morphology was studied on R2A agar medium (Fluka, Munich, Germany) by microscopy (Primo Star, Zeiss, Carl Zeiss Microscopy, Jena, Germany) of single colonies of each isolate (4× magnification). Subsequently, colonies were observed after 24 and 48 h using image processing software ZEISS Labscope (Carl Zeiss Microscopy, Jena, Germany). A Gram-staining analysis was performed according to Claus [68] using reagents Hucker's crystal violet, an iodine and safranin solution and 1-propanol to determine the Gram classification of each isolate. Each preparation was evaluated using Labscope software.

2.9. Transmission Electron Microscopy

Colony morphology of the isolates was observed by transmission electron microscopy (TEM). Data were imaged onto the screen using the software program digital Micrograph (Gatan GmbH, Munich, Germany). Both isolates were grown in liquid PYE medium [29] overnight at 30 °C. Afterwards, a negative staining technique was performed. 5 µL cell suspension were mixed with the same amount of diluted 0.1% phosphotungstic acid (3% stock, pH 7) and were transferred to a vaporized carbon mica for 1 min. Subsequently, the mica was briefly washed in demineralized water and transferred to a thin copper-coated grid (PLANO GmbH, Marburg, Germany). The coated grids were dried at room temperature and were examined by Jeol 1011 TEM (Georgia Electron Microscopy, Freising, Germany).

2.10. Determination of Temperature Optimum and Salt Tolerance

To quantify the temperature optimum, both isolates were grown in 4 mL PYE medium at 10, 20, 30, 35 and 40 °C at 180 rpm in a Infors HT shaker (Orbitron, Einsbach, Germany). The optical density of the cell suspensions was measured using the Ultraspec 3300 pro photometer (Amersham Pharmacia Biotec Europe GmbH, Munich, Germany) at a wavelength of 600 nm (OD_{600}). The starting OD_{600} of the cell cultures was 0.1.

For the determination of the salt tolerance, LVF1^T and LVF2^T were also inoculated in 4 mL PYE medium amended with 0, 5, 10, 20, 30 and 40 gL^{-1} NaCl. OD_{600} of the cell suspensions was set to 0.3 at the beginning of the experiment [2]. LVF1^T was incubated at 30 °C and 180 rpm in a Infors HT shaker (Orbitron, Einsbach, Germany). After the incubation period, the optical density of the isolates was measured at 600 nm. The differences between these two measurements were used for the determination of the salt tolerance [2]. All measurements were performed in biological replicates for each isolate. The collected data were illustrated with R studio version 4.0.2 [40] using the ggplot2 package [41].

2.11. Determination of Growth Kinetics

The growth kinetics in liquid cultures were measured with the cell growth quantifier (CGQuant 8.1) (Aquila Biolabs GmbH, Baesweiler, Germany) at 30 °C for 47 h. Pre-cultures were resuspended to a final OD_{600} of 0.1 in 25 mL PYE medium and were filled into 250 mL shake flasks. Afterwards, all flakes were mounted onto the CGQ sensor plate and were shaken for 47 h. The CGQ enables a dynamic approach of backscattered light measurement, implementing to follow the growth of the liquid cultures in real time [69]. All measurements were performed in biological replicates. All collected data were illustrated with R studio version 4.0.2 [40] using ggplot2 package [41].

2.12. Anaerobic Growth

First, cultures from aerobic growth were used to inoculate 5 mL pre-reduced PYE medium in Hungate tubes [70] with a final OD_{600} of 0.1. The cell suspensions were incubated at 30 °C. After five days, the pre-cultures were transferred to new Hungate tubes (final OD_{600} of 0.1) and were incubated at 30 °C. Potential growth was observed

in a time frame of 14 days. The determination of anaerobic growth was performed in biological replicates.

2.13. Metabolic Activity and Antibiotic Resistances

Metabolic activities were identified using API ZYM and API 20 NE tests. Both tests were performed by following the instructions given by the manufacturer (BioMérieux, Nuertingen, Germany). Catalase activity was determined using 3% H_2O_2 [71].

For the determination of antibiotic resistances, the following discs and strips (Oxoid, Wesel, Germany) were used: ampicillin (25 µg), chloramphenicol (30 µg), doxycycline (30 µg), kanamycin (30 µg/mL), oxytetracycline (30 µg), rifampicin (2 µg), streptomycin (10 µg), vancomycin (30 µg), erythromycin (0.015–256 µg), meropenem (0.002–32 µg), tetracycline (0.015–256 µg). To determine the response of both strains to the antibiotic a soft-agar (0.4% (*w*/*v*) agarose in PYE medium) overlay technique was used. 2.5 mL soft agar were used to inoculate the isolates with a final OD_{600} of 0.1. Afterwards, discs or strips were attached to the soft agar. All plates were incubated overnight at 30 °C.

3. Results

3.1. Enrichment of Caulobacteraceae from the Environment

To isolate organisms belonging to the family *Caulobacteraceae*, environmental samples were taken from plant material (frog's lettuce) from an oligotrophic pond (PM), surface water near pond algae (WSA), surface water near frog's lettuce (*Groenlandia densa*) (WSP), surface water of reed (WSR), surface water of Weende River entrance (WSW), mixed river stones (MRS), river stones (RS), pond water (PW), Weende River water (RW), eutrophic pond water (POW), surface water of stale eutrophic pond (PSW), and puddle water (PUW). These samples were used as inoculum for a 0.001% (*w*/*v*) peptone-based enrichment with and without methanol. Bacterial community compositions of the resulting cultures were analyzed based on the 16S rRNA gene amplicon analysis (Figure 1). Depending on the sample origin, we observed specific structures of the established bacterial community at order level. Cultures inoculated with oligotrophic samples always resulted in a similar composition of the microbial community regardless of the sampling site. There was also no significant difference between enrichment medium supplied with or without methanol at order level. Eutrophic water samples led to more diverse bacterial communities at order level with 105 different orders on average while oligotrophic water samples showed on average 10 different orders (Figure 1a). Detailed investigation of the alphaproteobacterial fraction revealed PW and PUW as the most promising samples for *Brevundimonas* isolation (Figure 1b). At genus level, a medium-dependent effect could be observed during the enrichments. Cultures enriched with methanol revealed *Brevundimonas* as the most dominant genus. The pond water (PW) sample showed the highest relative abundance of *Brevundimonas*. Cultures without methanol also contained genera of *Caulobacteracea*, but those were not predominant and were surpassed by families such as *Rhodospiriliaceae* and *Rhizobiaceae*. Cultures of eutrophic enrichment showed a more diverse composition (105 different orders on average) and a relatively homogeneous distribution within the Alphaproteobacteria with an average of 8 bacterial genera. Only the puddle water (PUW) sample exhibited higher abundance of *Brevundimonas* and *Caulobacter* and was therefore used for further bacterial isolations together with the PW enrichment.

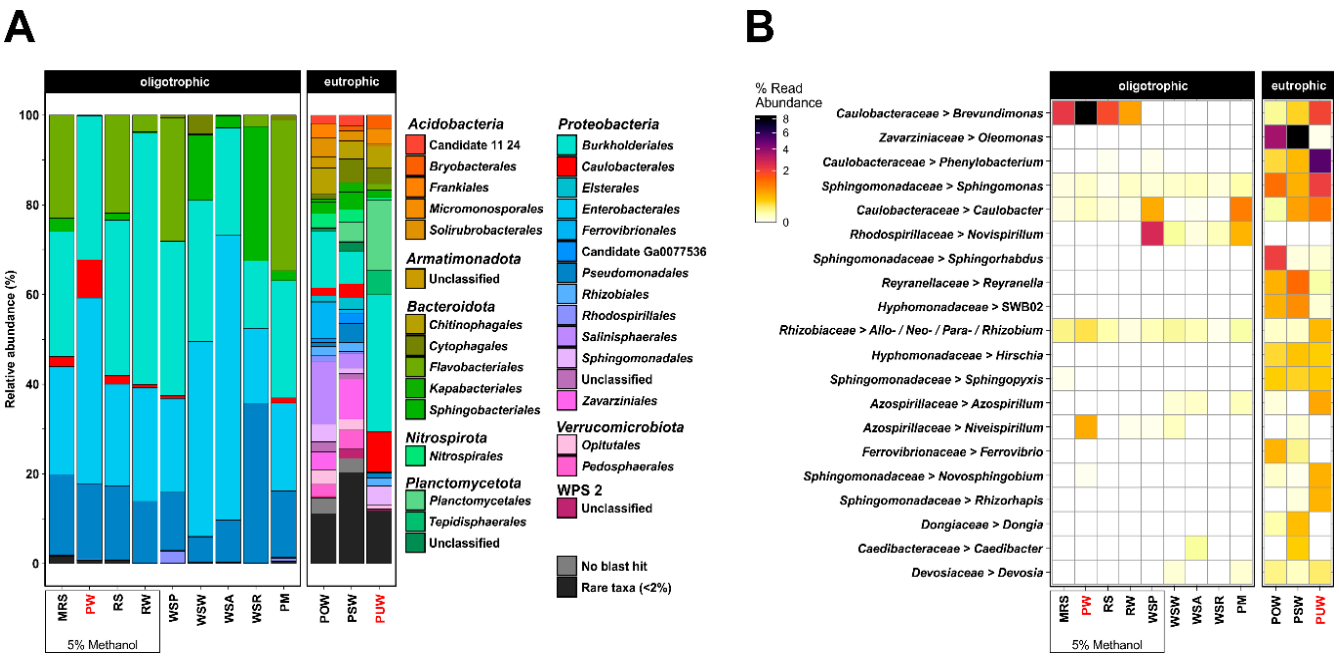

Figure 1. Amplicon-based analysis of the *Caulobacteraceae* enrichment from the different sampling sites. Relative abundance of bacterial family based on 16S rRNA gene analysis in cultures after enrichment with 0.001% (*w*/*v*) peptone and 0.001% (*w*/*v*) peptone with 5% (*v*/*v*) methanol. MRS, PW, RS and RW comprise the samples which were enriched with peptone and methanol. Red letters indicated enrichments of *Caulobacteraceae* used for isolation. (**A**) Each bacterial phylum depicted here comprises more than 2% relative abundance in at least one sample. (**B**) Relative read abundance of the top 20 enriched bacterial genera (including family) belonging to Alphaproteobacteria. Genera without cultured representatives and unclassified genera have been removed.

3.2. Caulobacteraceae Isolation from Enriched Environmental Samples

The different isolation attempts led to 37 individual isolates, which were all investigated by 16S rRNA gene sequencing (Supplementary Tables S2–S4). Three 16S rRNA gene sequences (LVF1, DAIF19 and LVF2) matched with those of known *Brevundimonas* strains (99.1 to 100% identity). Strains LVF1^T and DAIF19 derived from PW were identical, which was confirmed through Illumina sequencing (data not shown). Therefore, only the data from LVF1^T and LVF2^T were considered further. The remaining isolates did not belong to the *Caulobacteraceae* and were not further investigated. Examination of the remaining enrichment cultures resulted in 34 additional isolates. None of these could be assigned to the *Caulobacteraceae* family (Supplementary Table S5). Thus, we were able to isolate only members of *Brevundimonas* from the originally identified genera *Brevundimonas*, *Phenylobacterium* and *Caulobacter* of the family *Caulobacteraceae* (Figure 1b).

3.3. Phylogeny of LVF1^T and LVF2^T Based on Their Full Genome Sequence

In order to further classify the unique isolates LVF1^T and LVF2^T genome sequences were obtained. Both isolates were sequenced by Illumina and Oxford Nanopore technology. We were able to obtain high-quality closed genomes for both strains. The de novo hybrid genome assembly of LVF1^T, with an overall coverage (short- and long-reads) of 252.9-fold, resulted in one circular chromosome with a size of 3,550,773 bp and a GC-content of 67.04%. It encodes 3445 putative proteins, 58 rRNAs and 48 tRNAs. Assembly of strain LVF2^T exhibiting an overall sequence coverage of 245.4-fold resulted in a genome size of 3,984,955 bp with a GC-content of 67.79%. The chromosome encodes 3857 putative proteins, 57 rRNAs, 48 tRNAs. No plasmids and CRISPR regions were detected in both genomes. Genomic characteristics are listed in Table 2.

Table 2. Genome statistics of *Brevundimonas pondensis* sp. nov. LVF1^T and *Brevundimonas goettingensis* sp. nov. LVF2^T.

Features	*Brevundimonas pondensis* Sp. Nov. LVF1^T	*Brevundimonas goettingensis* Sp. Nov. LVF2^T
Genome size (bp)	3,550,773	3,984,955
GC content (%)	67.04	67.79
Coverage	252.9-fold	245.4-fold
CDS	3445	3857
rRNA genes	58	57
tRNA genes	48	48
ncRNA	4	3
CRISPR	0	0
Prophage(s)	2	1

Genome-based taxonomic assignment was performed with GTDB-Tk [60] and revealed an average nucleotide identity (ANI) for each strain of approximately 90% to the closest related species (ANI values 90.63-LVF1^T and 90.85-LVF2^T) (Supplementary Table S6). Additionally, the two isolates were confirmed as new species by employing the Type Strain Genome Sever (TYGS) [72]. ANI-analysis with known type strains of the genus *Brevundimonas* is shown in Figure 2 (data in Supplementary Table S7). No cluster formation with any other characterized *Brevundimonas* strain was observed. Close nucleotide sequence identity shares LVF1^T with *B. diminuta* NCTC 8545^T with 85.06% and *B. naejangsanensis* DSM 23858^T with 86.44%, and LVF2^T with *B. lenta* DSM 23960^T with 85.35% and *B. subvibrioides* ATCC 15264^T with 85.06% respectively. The genomes of strains LVF1^T and LVF2^T share a sequence identity of 84.55%.

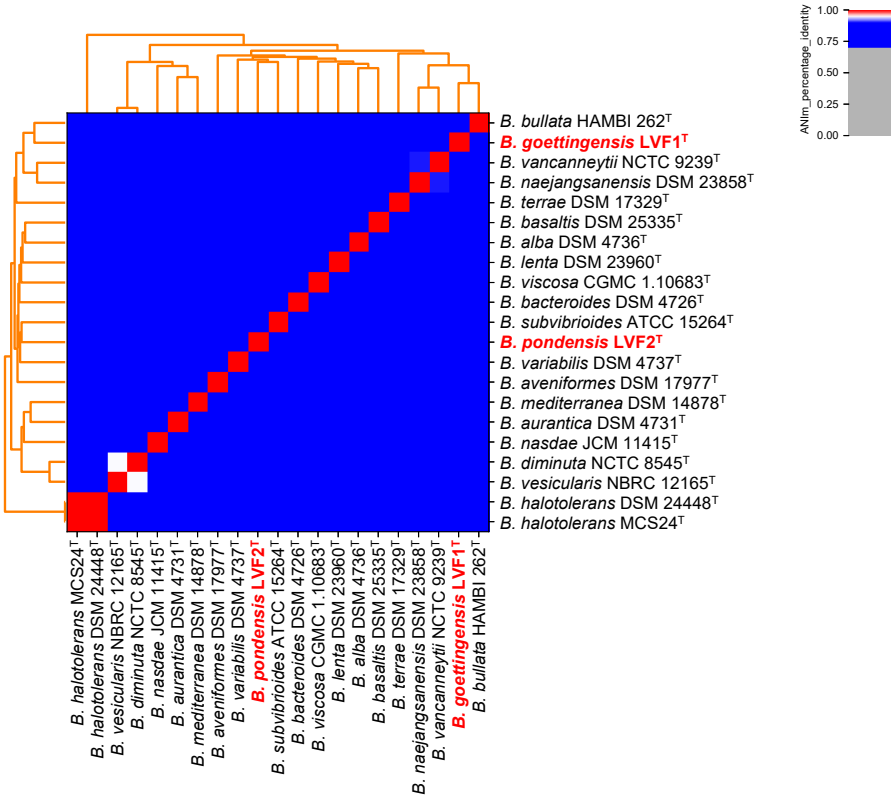

Figure 2. Phylogenetic analysis of *Brevundimonas pondensis* sp. nov. LVF1^T and *Brevundimonas goettingensis* sp. nov. LVF2^T. All available type strains (T) and representative strains (R) from the genus *Brevundimonas* were examined. Calculations were performed with pyani [61,73] using the ANIm method with standard parameters. Isolated strains LVF1^T and LVF2^T are depicted in bold red.

Thus, both strains are regarded as novel type strains of *Brevundimonas*, which we designated *Brevundimonas pondensis* sp. nov. LVF1^T and *Brevundimonas goettingensis* sp. nov. LVF2^T.

3.4. Identification of Prophage Regions

Prophage regions were initially analyzed with PHASTER [66], which revealed two putative prophage regions for *Brevundimonas pondensis* sp. nov. LVF1^T (region 1: 233,337–275,001; region 2: 330,414–348,898). The regions comprised 41.6 and 18.4 kb and were classified as incomplete (Supplementary Table S8). *Brevundimonas goettingensis* sp. nov. LVF2^T revealed one putative prophage region (245,339–261,838), comprising 16.5 kb. This was classified as intact despite its small size (Supplementary Table S9).

ProphageSeq [59] was applied for both strains and data of phage particle-packed dsDNA was mapped on the bacterial genomes and visualized (Figure 3). For LVF1^T, prophage reads accumulation associated with the PHASTER-predicted prophage regions, thereby indicating prophage activity. However, the coverage profile exhibits an uneven distribution of reads with a substantial coverage increase from base 254,001, followed by a constant decrease over 170 kbp following the replication direction of the genome (Figure 3). Thus, the mapping alone did not allow robust conclusions about the precise size of prophage 1 or prophage 2. Reads derived from assembled particle-packed dsDNA resulted in two contigs of 90,274 bp and 38,784 bp. The 38.8 kb contig was indicated as circular by the assembler. Sequence alignment with the host chromosome revealed that it represents the genome of prophage 2, including its *att* sites. Those were 73 bp long with one base deviation at position 15(TCAATCAAC-TAAGTa/gATTGAAAAGAATGGTGGACGCGACAGGGATTGAACCTGTGACCCCTACGA TGTCAACG). The integration locus of this prophage is a valine tRNA.

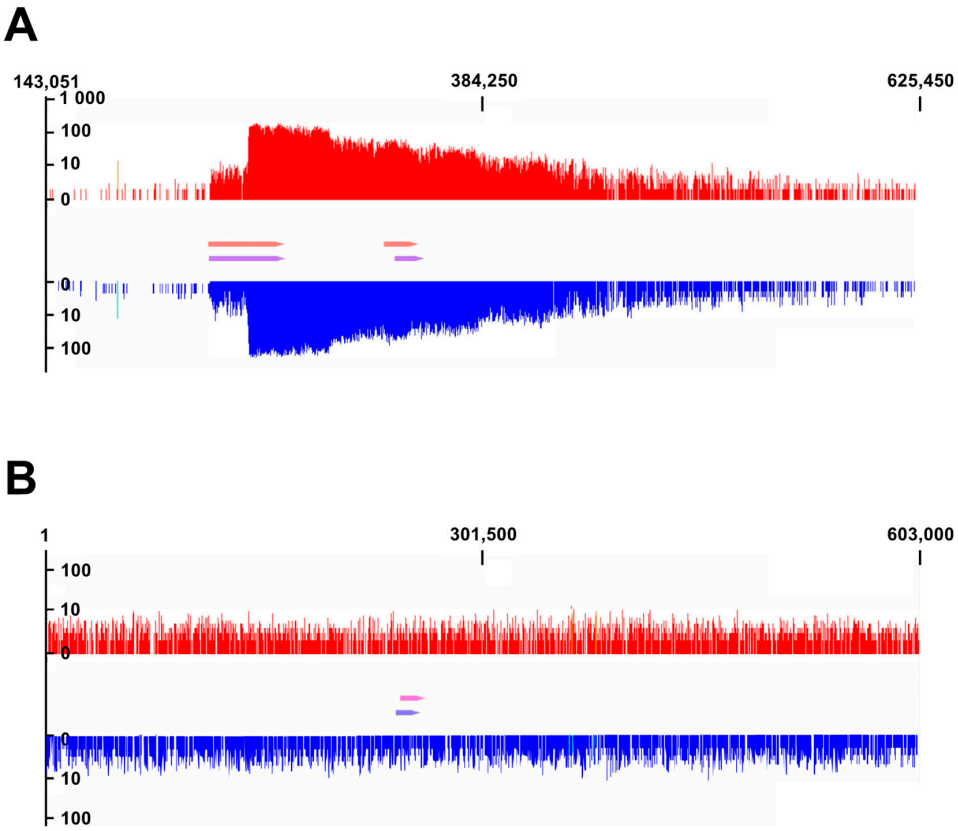

Figure 3. Read coverage profile of sequenced (**A**) LVF1^T and (**B**) LVF2^T prophages, mapped onto the corresponding host genome. The pinkish arrows depict the prophage regions, which were predicted with PHASTER [66]. In purple and blue are the experimentally verified prophage regions. Image A displays the read coverage of the LVF1^T genome between base 143,051 to 625,450 (482,399 kb). Image B displays the coverage of the LVF2^T genome between base 1 to 603,000 (629,999 kb).

The 90 kb contig represents mainly the sequence accumulation over the two prophage regions. The alignment with the host chromosome revealed the absence of prophage 2 in this genome fragment. Such an assembly result is only feasible if sequence reads are present crossing the prophage 2 region, which in turn is only possible if prophage 2 is excised from the host genome. Thus, this result indicates that prophage 2 is functional and capable to excise its viral genome from the host chromosome, circularize it, and package it in the procapsid.

Since it was not possible to obtain information on prophage 1, neither through sequence mapping nor read assembly, we aimed to narrow down its size by identifying its *att* sites. Due to the sequence accumulation of the particle-packaged DNA on its upstream boundary we suspected its *attL* site at position 233,401. Sequence analysis around this position and comparison against the entire genome of LVF1^T revealed an exact 58 bp long sequence at position 275,001 to 275,058 (TGGTGCGGGTGGGCCGGGCTCGAACCGGGCACTCCTCTCGGAACAGGATTTTGAATCCAG), representing the *attL/R* site of prophage 1. A leucine tRNA was identified as integration locus of prophage 1. The genome size of prophage 1 is 41,600 bp.

ProphageSeq of LVF2^T revealed no read accumulation neither at the predicted prophage location nor elsewhere on the bacterial chromosome. All phage particle-derived sequence reads mapped equally distributed over the entire host chromosome. Investigation of the surrounding gene annotations associated with the prophage prediction did not uncover any phage integration sites. However, the annotation enabled to adapt the boundaries of the predicted prophage region to 242,355 to 258,254, resulting in a final region size of 15,899 bp. Deduced proteins present in this region frequently encoded phage-related protein domains.

In conclusion, two prophage regions in the genome LVF1^T were identified and experimentally confirmed as particle-forming and capable of packing their genome. The prophage identified in the genome of LVF2^T is probably defective due to the random packing of the host chromosome.

3.5. Morphological Analysis of LVF1^T and LVF2^T

To get insights into strain-specific morphological characteristics, both colony morphology and cell morphology were analyzed. Colonies of LVF1^T, grown on PYE and R2A solid media, were colored grey-white, while colonies of strain LVF2^T were yellow. If grown overnight, the colony form of LVF1^T was elliptically shaped, convex and smooth and exhibited an average diameter of 0.8 mm. The same applies for LVF2^T colonies, which had an average diameter of approximately 1 mm (Supplementary Figure S2).

A Gram-staining of both isolates indicated a Gram-negative type (Supplementary Figure S3).

For transmission electron microscopy (TEM), liquid cultures (Supplementary Figure S4) of the isolates were used, which were grown in PYE medium and prepared with a negative staining technique. Single cells of LVF1^T were homogeneous in structure and size (Figure 4a,b). They were all motile, and stalks were not observed. The rod-shaped cells were approximately1.0 µm in length and 0.46 µm in width with one flagellum. Cells of LVF2^T showed evidence for asymmetrical cell division. A sessile mother cell with 1.7 µm long prostheca (stalk) and a daughter cell with a polar flagellum (Figure 4c,d) was observed. The cell bodies of the sessile cells were vibrio-shaped with a length of approximately 1.3 and 0.7 µm width while the cell body of the swarmer cell was elliptical and 1.6 µm in length and 0.6 µm in width. Furthermore, cells attached to each other with the terminal ends of their stalks were detected (Figure 4c). This documents the ability of LVF2^T cells to adhere to surfaces or form rosettes, which were frequently reported for three genera of *Caulobacteraceae* [3]. Thus, both isolates are motile, and LVF2^T is able to differentiate into two cell types.

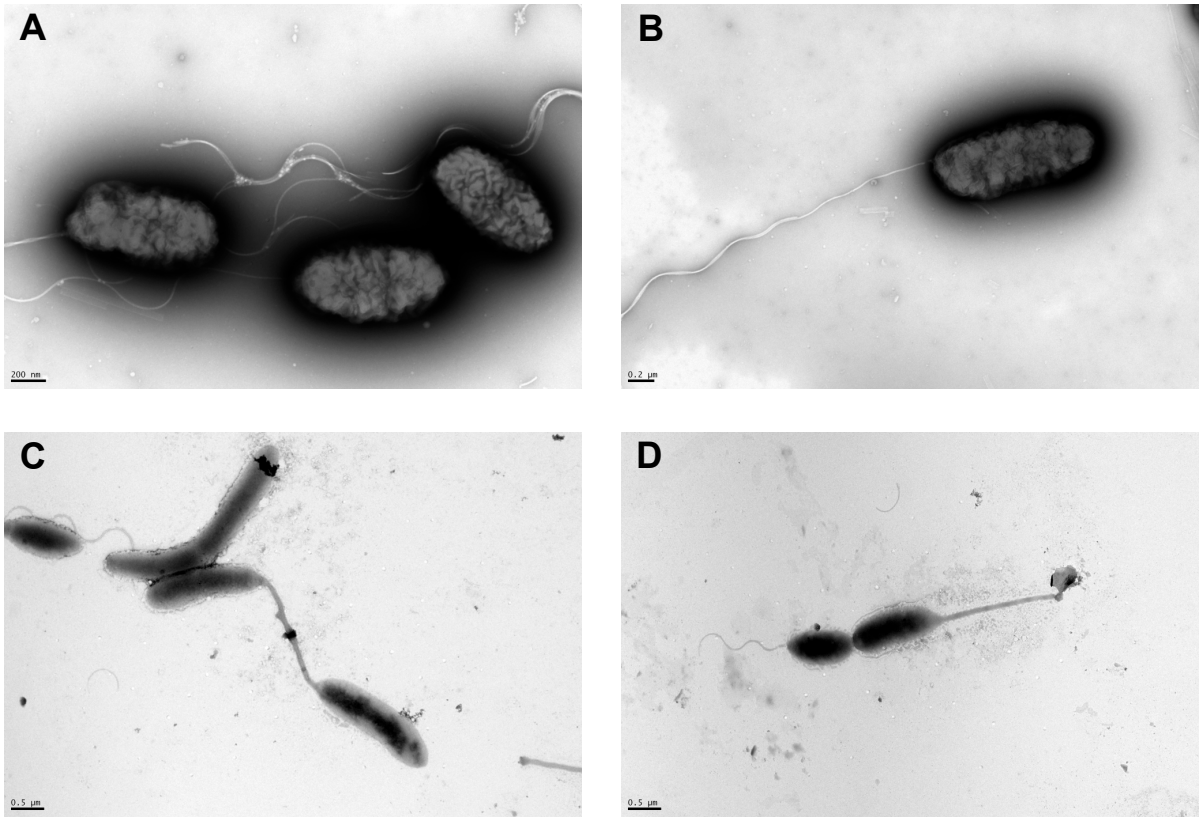

Figure 4. Transmission electron microscopy image of LVF1^T and LVF2^T. Micrographs show the general morphology of negatively stained cells of strains LVF1^T (**A**,**B**), and LVF2^T (**C**,**D**). LVF1^T at 30 °C was grown in liquid PYE medium for 24 h and LVF2^T in the same medium for 48 h.

3.6. Physiological Characterization

The physiological properties and the metabolic potential of the new proposed type strains were characterized by growth and metabolic experiments. Additionally, an antibiogram was generated to reveal the antibiotic resistance potential of both strains. LVF1^T was able to grow at a temperature range between 10 and 40 °C and LVF2^T between 10 and 35 °C. Both strains are mesophiles as their growth optimum was at 30 °C. LVF1^T reached higher cell densities at 30 °C than LVF2^T (OD_{600} of 1.533 and 0.887, respectively; Figure 5a).

Both strains were able to grow in the presence of up to 4% (*w*/*v*) NaCl in PYE medium. The salt optimum of LVF1^T was between 0–1% (*w*/*v*) NaCl and that of LVF2^T between 0–0.5% (*w*/*v*) (Figure 5b).

Growth kinetics of both strains were determined under optimal salt and temperature conditions (Figure 5c). Under the experimental conditions, the lag phase of LVF1^T lasted for approximately three hours and that of LVF2^T for approximately eight hours. The duration of the exponential growth phase was 7.5 h for LVF1^T and 8 h for LVF2^T and thus almost identical between both strains. LVF1^T has a doubling time of 146 min and LVF2^T of 165 min. The growth rate µ of LVF1^T is 0.28 h^{-1} and 0.25 h^{-1} for LVF2^T. However, the transient phase of LVF2^T was extended in comparison to LVF1^T and resulted in a higher final cell density of LVF2^T. In addition, the ability for anaerobic growth was also investigated. Therefore, aerobic pre-cultures were gassed with nitrogen and used as inoculum for cultures in Hungate tubes filled with anaerobic PYE medium. Anaerobic cultures were inoculated with OD_{600} of 0.1 and incubated at optimal temperature without addition of sodium chloride for 14 days. Cell growth of LVF1^T increased almost eightfold, resulting in a final OD_{600} of 0.765. LVF2^T showed no growth under these conditions.

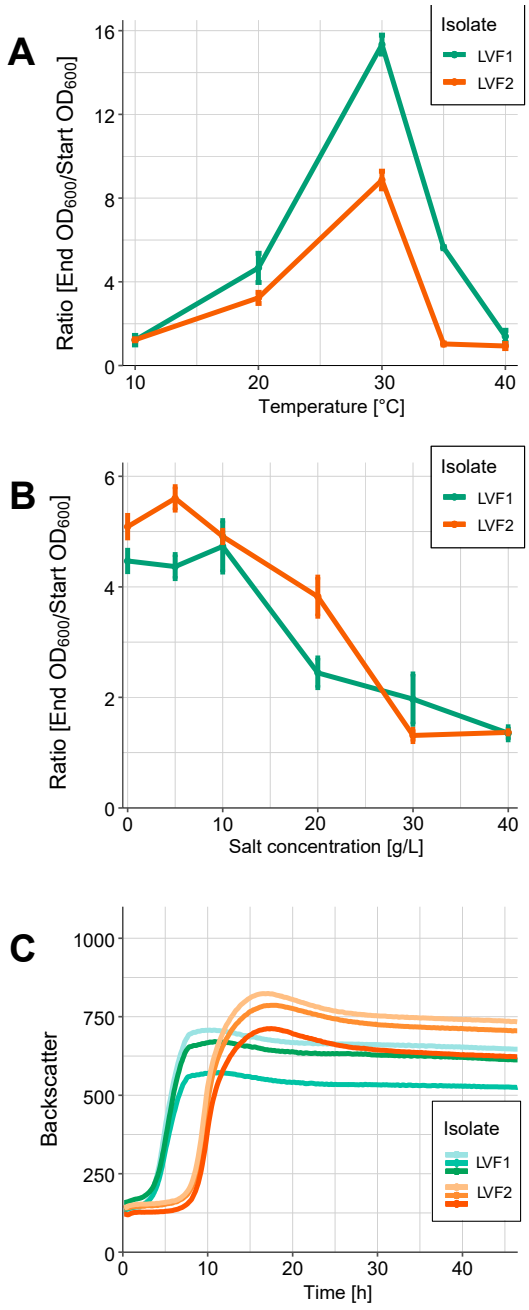

Figure 5. Growth analysis of LVF1^T and LVF2^T. (**A**) Growth of LVF1^T (green) and LVF2^T (orange) in 4 mL test tubes at different temperatures inoculated in PYE medium and incubated for 24 h (LVF2^T) and 16 h (LVF1^T) at 180 rpm in a Infors HT shaker (Orbitron, Einsbach, Germany). (**B**) Samples were inoculated in PYE medium and incubated for 30 h (LVF2^T, orange) and 24 h (LVF1^T, green) at 180 rpm. (**C**) Growth analysis of LVF1^T (green) and LVF2^T (orange) at optimum temperature (30 °C) in 25 mL PYE medium. Measurements were performed in triplicate and for (**A**,**B**) the standard deviation is shown as error bars, for (**C**) in different shades of green or orange.

The metabolic potential of both isolates was analyzed by using the API ZYM and the API 20 NE tests. In this way, forty different enzyme activities were determined for both isolates. Both showed no enzymatic activities in 27 cases. Ten were present in both strains, which included alkaline phosphatase, esterase, lipase, leucine arylamidase, trypsin, acid phosphatase, Naphthol-and AS-BI-phosphohydrolase, as well as the ability to utilize esculin, D-maltose and capric acid. Three enzyme activities were strain specific. Valine arylamidase or α-chymotrypsin were detected in LVF2^T whereas the activity of

β-glucosidase was observed for LVF1^T. In addition, both strains were catalase positive. Oxidase reagent from API ZYM test showed oxidase activity for both isolates. A general overview of all enzyme activities is listed in Table 3.

Table 3. Differential phenotypic characteristics of strains LVF1^T and LVF2^T and phylogenetically related species *B. diminuta* NCTC 9239^T, *B. lenta* DSM 23960^T, *B. naejangsanensis* DSM 23858^T, and *B. subvibrioides* ATCC 15264^T. Taxa: 1, strain LVF1^T; 2, strain LVF2^T; 3, *B. diminuta* NCTC 9239^T (data from [9] BacDive [74] accessed on 12 January 2021); 4, *B. lenta* DSM 23960^T (data from [10]); 5, *B. naejangsanensis* DSM 23858^T (data from BacDive [74] accessed on 12 January 2021); 6, *B. subvibrioides* ATCC 15264^T (data from [7]). +, Positive; −, negative; v, some strains showed activity; n/a, not available.

Characteristics	***B. pondensis* LVF1^T**	***B. goettingensis* LVF2^T**	***B. diminuta* NCTC 9239^T**	***B. lenta* DSM 23960^T**	***B. naejangsensis* DSM 23858^T**	***B. subvibrioides* ATCC 15264^T**
Source of isolation	Oligotrophic pond water	Puddle water	Water	Soil	Soil	Pond water
Colony pigmentation	Gray-white (PYE/R2A)	Yellow (PYE/R2A)	None (NA)	Grayish-yellow (NA)	Grayish-yellow (TSA)	Dark orange (PYE)
Stalk formation	−	+	n/a	n/a	−	+
Anaerobic growth	+	−	−	−	+	−
Temperature (°C)						
Range	10–40	10–40	n/a	4–34	4–50	n/a
Optimum	30	30	28	25	30	30
NaCl (g/L)						
Range	0–40	0–40	n/a	0–10	0–40	0–20
Optimum	0–10	0–5	n/a	0	5	20
Enzymatic activity						
Alkaline phosphatase	+	+	+	+	+	n/a
Esterase	+	+	+	+	+	n/a
Esterase lipase	+	+	+	+	+	n/a
Lipase	−	−	−	−	−	n/a
Leucine arylamidase	+	+	+	+	+	*v*
Valine arylamidase	+	−	−	−	−	−
Cysteine arylamidase	−	−	−	−	−	n/a
Trypsin	+	+	+	+	+	n/a
α-Chymotrypsin	+	−	+	−	+	n/a
Acid phosphatase	+	+	+	+	+	n/a
Naphthol-AS-BI-phosphohydrolase	+	+	+	+	+	n/a
α-Galactosidase	−	−	−	−	−	n/a
β-Galactosidase	−	−	−	−	−	n/a
β-Glucuronidase	−	−	−	−	−	n/a
α-Glucosidase	−	−	−	n/a	−	n/a
β-Glucosidase	−	+	−	n/a	−	n/a
N-Acetyl-β-glucosaminidase	−	−	−	−	−	n/a
α-Mannosidase	−	−	−	−	−	n/a
α-Fucosidase	−	−	−	−	−	n/a
Utilization of						
Potassium nitrate	−	−	−	n/a	−	−
L-Tryptophane	−	−	−	n/a	−	n/a
D-Glucose (fermentation)	−	−	−	n/a	−	n/a
L-Arginine	−	−	−	n/a	−	−
Urea	−	−	−	n/a	−	n/a

Table 3. *Cont.*

Characteristics	*B. pondensis* LVF1^T	*B. goettingensis* LVF2^T	*B. diminuta* NCTC 9239^T	*B. lenta* DSM 23960^T	*B. naejangsensis* DSM 23858^T	*B. subvibrioides* ATCC 15264^T
Esculin/ferric citrate	+	+	−	n/a	−	n/a
Gelatin	−	−	−	n/a	−	n/a
4-Nitrophenyl-β-D-galactopyranoside	−	−	−	n/a	−	n/a
D-Glucose (assimilation)	−	−	−	−	−	+
L-Arabinose	−	−	−	−	−	*v*
D-Mannose	−	−	−	−	−	−
D-Mannitol	−	−	−	−	−	n/a
N-Acetyl-D-glucosamine	−	−	−	−	−	n/a
D-Maltose	+	+	−	−	−	+
Potassium gluconate	−	−	−	−	−	n/a
Capric acid	+	+	−	n/a	−	n/a
Adipic acid	−	−	−	n/a	−	n/a
Malic acid	−	−	−	n/a	+	n/a
Trisodium citrate	−	−	−	n/a	−	n/a
Phenylacetic acid	−	−	−	n/a	−	n/a
Oxidase	+	+	+	n/a	+	+
Catalase	+	+	+	n/a	+	+
Resistance to						
Ampicillin	−	−	+	+	+	n/a
Chloramphenicol	−	−	−	−	−	n/a
Doxycycline	−	−	−	n/a	n/a	n/a
Erythromycin	+	+	−	n/a	n/a	n/a
Kanamycin	−	−	−	−	−	n/a
Meropenem	+	+	n/a	n/a	n/a	n/a
Oxytetracycline	−	−	n/a	n/a	n/a	n/a
Rifampicin	−	−	n/a	n/a	n/a	n/a
Streptomycin	+	+	n/a	n/a	−	−
Tetracycline	+	+	−	−	−	n/a
Vancomycin	+	+	−	n/a	n/a	n/a
G + C %	67.04	67.79	67	68.7	67	67

In bold: Sorted by categories.

The antibiogram (Supplementary Figure S5) revealed that both isolates are resistant to erythromycin (LVF1^T 2 µg/disc and LVF2^T 4 µg/disc), meropenem (up to 2 µg/disc), streptomycin (10 µg/disc), tetracycline (up to 1 µg/disc), and vancomycin (30 µg/disc). Resfams in silico analysis [67] indicated genes present coding for an ABC transporter using erythromycin as substrate, β-lactamases for meropenem inactivation, tetracycline inactivation enzyme (*tetX*), and RND antibiotic efflux systems. The latter could be responsible for the aminoglycoside tolerance (Supplementary Tables S10 and S11).

B. pondensis sp. nov. LVF1^T and *B. goettingensis* sp. nov. LVF2^T show a different antibiogram compared to their phylogenetically closest relatives. Both are not resistant against ampicillin and comparing them with *B. diminuta* NCTC 9239^T, *B. lenta* DSM 23960^T and *B. naejangsanensis* DSM 23858^T but both possess a streptomycin and tetracycline resistance (Table 3).

4. Discussion

The aim of this study was to isolate new host strains of the *Caulobacteraceae* family to access the associated phage diversity present in the corresponding environments. This was realized successfully from environmental enrichment cultures with suitable amounts of *Caulobacterales* members. However, WSW (water surface of Weende River entrance), WSA (water surface of algae), and WSR (water surface of reed) revealed no or almost no members of this order. This was not expected as these were plant-associated samples, and members of the order *Caulobacterales* are known to be associated with plant material [8]. Some plants

such as reed (*Phragmites australis*) are able to increase microbial degradation due to oxygen availability but also the presence of certain microorganisms depends on the compounds released by reed [75]. WSW is the entrance of the river Weende. Here, the flow rate of the water is fast and would require strong adhesion of the stalked cells [3]. This might explain the lack of isolates from *Caulobacterales*. Enrichments from PW (oligotrophic pond water) or PUW (puddle water) revealed significant presence of *Caulobacterales*. These promising samples differed from the samples lacking *Caulobacterales* mainly in their standing waters, which are also at risk of drying out. Thus, the ability of *Caulobacterales* to withstand such seasonal fluctuations might be the crucial factor. Fazi et al. (2008) reported that the *Caulobacterales* are among the first to colonize a habitat after rehydration, which is often the case in Italian river sediments after heavy rain [76]. The authors of this study hypothesized that this characteristic is due to the ability of many members to form rigid biofilms [76].

The promising PW and PUW samples finally led to the isolation of the strains described here, which are associated with *Brevundimonas* based on their 16S rRNA gene sequence. Comparison of the whole genome with the representative type strains of this genus revealed LVF1^T and LVF2^T to represent new species (Figure 2). Apart from the genome, *Brevundimonas pondensis* sp. nov. LVF1^T and *Brevundimonas goettingensis* sp. nov. LVF2^T also show phenotypic differences. The colonies of LVF1^T are grayish-white, while that of LVF2^T are yellow. The origin of the coloration may be due to the production of carotenoids, which some *Brevundimonas* species are capable to synthesize [3]. In the genome of LVF1^T (white colony) we could not identify any putative genes for carotenoid biosynthesis, but we could in the genome of LVF2^T (yellowish colony) (Supplementary Tables S12 and S13).

Both strains exhibited distinct cell morphologies. LVF2^T showed prosthecate and non-prosthecate vibrio shape cell types, whereas LVF1^T showed only motile cells with polar flagella. The ability to divide asymmetrically, resulting in the distinct cell types, is rarely observed in *Brevundimonas*, i.e., in *B. subvibrioides* ATCC 15264^T [7]. It is more frequently observed in *Caulobacter* [4,5]. Since LVF2^T exhibits characteristics of both genera, its scientific importance goes beyond its service as a phage host strain.

Physiological analyses revealed that both strains grow optimally at 30 °C, which is in agreement with the literature, as freshwater and terrestrial members of *Cauolobactereacae* grow optimally at 30 °C [7,9,77]. Initial growth experiments showed that LVF1^T achieves higher cell densities than LVF2^T. However, this apparent advantage could be due to the conditions used. These experiments were conducted in test tubes with 4 mL medium under vigorous shaking. The still suboptimal aeration affected LVF2^T more than LVF1^T, since LVF2^T unlike LVF1^T is only capable of aerobic growth. Growth in conical flasks with optimal aeration resulted in an opposite behavior as LVF2^T reached higher densities than LVF1^T under these conditions (Figure 5c). LVF2^T also presented its competitive advantage at extreme temperatures such as 4 °C. It showed detectable growth after nine days, whereas LVF1^T required 16 days (data not shown). The data regarding growth in different NaCl concentrations correlate well with those known from literature for this genus [2,78] and are in good agreement with parameters frequently observed in environments from which both strains originated [78].

Both strains showed only minor differences with respect to the tested metabolic activities. Enzyme activity of valine arylamidase and α-chymotrypsin is missing in LVF2^T, whereas β-glucosidase activity is present. These experimental data were confirmed by genetic analysis using the KEGG pathway database (Supplementary Tables S14 and S15). The β-glucosidase activity of LVF2^T is significant, and to our knowledge, it has only been observed previously in *B. staleyi* [17]. Both isolates were oxidase- and catalase-positive, which is expected for the *Caulobacteraceae* family [7,9,77].

Antibiograms and the in silico investigations of both strains revealed a resistance potential with respect to medically relevant antibiotics. These results might be an indication of how far antibiotic contamination of our environment has progressed [79], especially as both isolates were isolated from protected habitats. However, this could also indicate that presence of antibiotic resistance genes are a natural phenomenon, as the presented

isolates originate from a complex environment where they likely face natural producers of antibiotics, e.g., *Streptomyces* [80]. In the future, analysis of the sample material with respect to content of different antibiotics should be considered to obtain clarity on this point.

The prophage potential of both strains was of particular interest as both isolates represent potential host systems for studying phage diversity in the environment. Our data confirmed that bioinformatical prediction using PHASTER [66] was imprecise. Since the prediction is mainly based on protein similarity to known phage proteins, the results indicate that phage diversity associated with Caulobacterales is not yet well understood. ProphageSeq of LVF1^T showed that read mappings are distributed far downstream of the identified prophages. This is likely related to the packaging mechanisms of the prophage. One of them may frequently recruit the packaging sites (*pac*) located in the prophage instance and translocate the chromosome constantly and unidirectionally into the prophage heads. The fadeout of reads reflects the likelihood of the phage translocase holding on to the initially grabbed dsDNA strand. We assume that both prophages of LVF1^T are able of forming phage particles. Prophage 2 due to the assembly of its genome and Prophage 1 as we could observe particle-packed sequence reads upstream the chromosomal *pac* site. In LVF2^T, we detected that the prophage randomly packs the host chromosome into its particles. This prophage is damaged or already domesticated by the host to perform a function required by the host. Similar cases are known for the PBSX prophages of *Bacillus pumilus* (Jin et al., 2014) and the gene transfer agents of *Rhodobacteraceae* [81].

In conclusion, although we did not manage to isolate a strain of the genus *Caulobacter*, we recovered two interesting isolates. LVF2 shows significant morphological similarity to the *Caulobacter* genus, although assigned as *Brevundimonas*. As a host strain, it might unite the viromes of both genera and be of particular value for the investigation of the environmental phage diversity. The presence of only a few prophages in the genome makes them even more attractive for this purpose. It is known that prophages can protect their host from infections of related and unrelated viruses [82–84]. The good manageability of the strains with respect to culture conditions make them promising candidates for future model organisms. For these reasons, we share the isolated strains with the scientific community and make them available with the help of the German Collection of Microorganisms and Cell Cultures GmbH (DSMZ), the Culture Collection University of Gothenburg (CCUG), and the Belgian Coordinated Collections of Microorganisms (BCCM/LMG).

4.1. Description of Brevundimonas Pondensis sp. nov.

Brevundimonas pondensis (pon. den'sis. N.L. fem. adj. *pondensis* pertaining to pond (51°33′57″ N 9°57′20″ E, collected on 6 September 2018), the source from which the type strain was isolated.

Cells are Gram-negative and rod-shaped (1.0 × 0.46 µm). Motile by means of a single polar flagellum. Colonies on PYE and R2A are round, slightly convex smooth and grayish-white with 0.8 mm diameter after 24 h of incubation at 30 °C. Growth occurs between 10 and 40 °C. Growth occurs in the presence of 0–4% (*w*/*v*) NaCl, with an optimum in the presence of 0–1% (*w*/*v*) NaCl. Growth occurs under anaerobic conditions. Susceptible to ampicillin, chloramphenicol, doxycycline, kanamycin, oxytetracycline, rifampicin, but not to erythromycin, meropenem, streptomycin, tetracycline, and vancomycin. In assays with the API 20 NE system, it showed the utilization of esculin, D-maltose, and capric acid. In assays with the API ZYM system, alkaline phosphatase, esterase, esterase lipase, leucine arylamidase, valine arylamidase, trypsin, α-Chymotropsin, acid phosphatase, and naphthol-AS-BI-phosphohydrolase are present. Other phenotypic characteristics are given in Table 3.

The type strain, LVF1^T (=DSM 112304^T = CCUG 74982^T = LMG 32096^T), was isolated from an oligotrophic pond located in Göttingen, Germany. The DNA G + C content of the type strain is 67.04 mol% (determined by PGAP).

4.2. Description of Brevundimonas Goettingensis sp. nov.

Brevundimonas goettingensis (goet.tin.gen'sis N.L. fem. adj. *goettingensis* pertaining to Göttingen city (51°33′27″ N 9°56′40″ E, collected on 24 September 2018) where the type strain was isolated).

Stalked cells are Gram-negative and vibrio-shaped (1.3 × 0.7 µm), the swarmer cells are elliptical (1.0 × 0.6 µm). Motile by means of a single polar flagellum. Colonies on PYE and R2A are elliptical, slightly convex, smooth and yellow with 1.0 mm diameter after 48 h of incubation at 30 °C. Growth occurs between 10 and 40 °C. Growth occurs in the presence of 0–4% (*w*/*v*) NaCl, with an optimum in the presence of 0–0.05% (*w*/*v*) NaCl. Susceptible to ampicillin, chloramphenicol, doxycycline, kanamycin, oxytetracycline, rifampicin, but not to erythromycin, meropenem, streptomycin, tetracycline, and vancomycin. In assays with the API 20 NE system, it showed the utilization of esculin, D-maltose, and capric acid. In assays with the API ZYM system, alkaline phosphatase, esterase, esterase lipase, leucine arylamidase, trypsin, acid phosphatase, naphthol-AS-BI-phosphohydrolase, and β-Glucosidase are detected. Other phenotypic characteristics are given in Table 3.

The type strain LVF2^T (=DSM 112305^T = CCUG 74983^T = LMG 32097^T), was isolated from an oligotrophic pond located in Göttingen, Germany. The DNA G + C content of the type strain is 67.79 mol% (determined by PGAP).

Supplementary Materials: The figures and tables are available online at https://www.mdpi.com/article/10.3390/applmicrobiol1010005/s1, Figure S1: Visualization of BLASTKoala output for both isolates, Figure S2: Phenotype of both isolates, Figure S3: Colony morphology of both isolates, Figure S4: Gram staining of both isolates, Figure S5: Analysis of antibiotic resistances of both isolates, Table S1: CheckM evaluation of both isolates, Table S2: Metadata of sampling sites, Table S3: ASV counts and taxonomic assignments, Table S4: Assigned ASV sequences after bioinformatic processing, Table S5: Identification results of bacterial isolates from enriched environmental sampling sites, Table S6: GTDB-Tk result of both isolates, Table S7: Phylogenetic analysis of both isolates, Table S8: PHASTER analysis of *Brevundimonas pondensis* LVF1^T, Table S9: PHASTER analysis of *Brevundimonas goettingensis* LVF2^T, Table S10: Resfams predicition of *Brevundimonas pondensis* LVF1^T, Table S11: Resfams prediction of *Brevundimonas goettingensis* LVF2^T, Table S12: List of putative biosynthetic gene clusters in *Brevundimonas pondensis* LVF1^T, Table S13: List of putative biosynthetic gene clusters in *Brevundimonas goettingensis* LVF2^T, Table S14: KEGG Mapper Reconstruction Result of *Brevundimonas pondensis* LVF1^T, Table S15: KEGG Mapper Reconstruction Result of *Brevundimonas goettingensis* LVF2^T.

Author Contributions: Conceptualization, I.F., R.H. and R.D.; experiments, I.F., A.K. and H.N.; data analysis, I.F., D.S. and R.H.; writing, I.F. and R.H. All authors interpreted the results, edited and reviewed the manuscript, and approved submission of the manuscript. All authors have read and agreed to the published version of the manuscript.

Funding: This research received no external funding.

Institutional Review Board Statement: Not applicable.

Informed Consent Statement: Not applicable.

Data Availability Statement: The 16S rRNA gene amplicon raw reads were deposited to the National Center for Biotechnology Information Sequence Read Archive (SRA) under the accession numbers SRR13285071 (eutrophic pond), SRR13285072 (frog's lettuce (*Groenlandia densa*)), SRR13285073 (surface water of reed), SRR13285074 (surface water near pond algae), SRR13285075 (surface water close from Weende River entrance), SRR13285076 (surface water near frog's lettuce), SRR13285077 (river water), SRR13285078 (river stones), SRR13285079 (puddle water), SRR13285080 (surface water of stale eutrophic pond), SRR13285081 (pond water), and SRR13285082 (mixed river stones). As well with the BioProject number PRJNA686076. The whole-genome shotgun project of *Brevundimonas pondensis* sp. nov. LVF1^T and *Brevundimonas goettingensis* sp. nov. LVF2^T has been deposited at GenBank under the accession numbers CP062006 and CP062222, respectively and the BioProject accession number PRJNA664909 and PRJNA664918. BioSample accession numbers are SAMN16237053 and SAMN16237121. The raw reads have been deposited in the NCBI SRA database with the accession

numbers SRR12931068 and SRR12951179 (Oxford Nanopore) and SRR12931069 and SRR12951180 (Illumina MiSeq).

Acknowledgments: We thank Anja Poehlein for sequencing, Melanie Heinemann and Mechthild Bömeke for technical assistance and Michael Hoppert for the support of TEM-imaging of both isolates. We acknowledge the support by the Open Access Publication Funds of the University of Göttingen.

Conflicts of Interest: The authors declare no conflict of interest.

References

1. Henrici, A.T.; Johnson, D.E. Studies of Freshwater Bacteria: II. Stalked Bacteria, a New Order of Schizomycetes. *J. Bacteriol.* **1935**, *30*, 61–93. [CrossRef]
2. Abraham, W.-R.; Strompl, C.; Meyer, H.; Lindholst, S.; Moore, E.R.B.; Christ, R.; Vancanneyt, M.; Tindall, B.J.; Bennasar, A.; Smit, J.; et al. Phylogeny and Polyphasic Taxonomy of *Caulobacter* Species. Proposal of *Maricaulis* gen. nov. with *Maricaulis maris* (Poindexter) comb. nov. as the Type Species, and Emended Description of the Genera *Brevundimonas* and *Caulobacter*. *Int. J. Syst. Bacteriol.* **1999**, *49*, 1053–1073. [CrossRef] [PubMed]
3. Abraham, W.-R.; Rohde, M.; Bennasar, A. The family *Caulobacteraceae*. In *The Prokaryotes*; Rosenberg, E., DeLong, E.F., Lory, S., Stackebrandt, E., Thompson, F., Eds.; Springer: Berlin/Heidelberg, Germany, 2014; pp. 179–205. ISBN 978-3-642-30197-1.
4. Staley, J.T. Prosthecomicrobium and Ancalomicrobium: New Prosthecate Freshwater Bacteria. *J. Bacteriol.* **1968**, *95*, 1921–1942. [CrossRef]
5. Jin, L.; Lee, H.-G.; Kim, H.-S.; Ahn, C.-Y.; Oh, H.-M. *Caulobacter daechungensis* sp. nov., a Stalked Bacterium Isolated from a Eutrophic Reservoir. *Int. J. Syst. Evol. Microbiol.* **2014**, *63*, 2559–2564. [CrossRef]
6. Stove, J.L.; Stanier, R.Y. Cellular Differentiation in Stalked Bacteria. *Nature* **1962**, *196*, 1189–1192. [CrossRef]
7. Poindexter, J.S. Biological Properties and Classification of the *Caulobacter* Group. *Bacteriol. Rev.* **1964**, *28*, 231–295. [CrossRef]
8. Wilhelm, R.C. Following the Terrestrial Tracks of *Caulobacter*—Redefining the Ecology of a Reputed Aquatic Oligotroph. *ISME J.* **2018**, *12*, 3025–3037. [CrossRef]
9. Segers, P.; Vancanneyt, M.; Pot, B.; Torck, U.; Hoste, B.; Dewettinck, D.; Falsen, E.; Kersters, K.; De Vos, P. Classification of *Pseudomonas diminuta* Leifson and Hugh 1954 and *Pseudomonas vesicularis* Büsing, Döll, and Freytag 1953 in *Brevundimonas* gen. nov. as *Brevundimonas diminuta* comb. nov. and *Brevundimonas vesicularis* comb. nov., Respectively. *Int. J. Syst. Evol. Microbiol.* **1994**, *44*, 499–510. [CrossRef]
10. Yoon, J.H.; Kang, S.J.; Oh, H.W.; Lee, J.S.; Oh, T.K. *Brevundimonas kwangchunensis* sp. nov., Isolated from an Alkaline Soil in Korea. *Int. J. Syst. Evol. Microbiol.* **2006**, *56*, 613–617. [CrossRef]
11. Ryu, S.H.; Park, M.; Lee, J.R.; Yun, P.-Y.; Jeon, C.O. *Brevundimonas aveniformis* sp. nov., a Stalked Species Isolated from Activated Sludge. *Int. J. Syst. Evol. Microbiol.* **2007**, *57*, 1561–1565. [CrossRef] [PubMed]
12. Estrela, A.B.; Abraham, W.R. *Brevundimonas vancanneytii* sp. nov., Isolated from Blood of a Patient with Endocarditis. *Int. J. Syst. Evol. Microbiol.* **2010**, *60*, 2129–2134. [CrossRef] [PubMed]
13. Choi, J.H.; Kim, M.S.; Roh, S.W.; Bae, J.W. *Brevundimonas basaltis* sp. nov., Isolated from Black Sand. *Int. J. Syst. Evol. Microbiol.* **2010**, *60*, 1488–1492. [CrossRef] [PubMed]
14. Vu, H.T.T.; Manangkil, O.E.; Mori, N.; Yoshida, S.; Nakamura, C. Post-Germination Seedling Vigor under Submergence and Submergence-Induced SUB1A Gene Expression in Indica and Japonica Rice (*Oryza sativa* L.). *Aust. J. Crop Sci.* **2010**, *4*, 264–272. [CrossRef]
15. Wang, J.; Zhang, J.; Ding, K.; Xin, Y.; Pang, H. *Brevundimonas viscosa* sp. nov., Isolated from Saline Soil. *Int. J. Syst. Evol. Microbiol.* **2012**, *62*, 2475–2479. [CrossRef] [PubMed]
16. Tsubouchi, T.; Koyama, S.; Mori, K.; Shimane, Y.; Usui, K.; Tokuda, M.; Tame, A.; Uematsu, K.; Maruyama, T.; Hatada, Y. *Brevundimonas denitrificans* sp. nov., a Denitrifying Bacterium Isolated from Deep Subseafloor Sediment. *Int. J. Syst. Evol. Microbiol.* **2014**, *64*, 3709–3716. [CrossRef] [PubMed]
17. Abraham, W.-R.; Estrela, A.B.; Nikitin, D.I.; Smit, J.; Vancanneyt, M. *Brevundimonas halotolerans* sp. nov., *Brevundimonas poindexterae* sp. nov. and *Brevundimonas staleyi* sp. nov., Prosthecate Bacteria from Aquatic Habitats. *Int. J. Syst. Evol. Microbiol.* **2010**, *60*, 1837–1843. [CrossRef]
18. Tóth, E.; Szuróczki, S.; Kéki, Z.; Kosztik, J.; Makk, J.; Bóka, K.; Spröer, C.; Márialigeti, K.; Schumann, P. *Brevundimonas balnearis* sp. nov., Isolated from the Well Water of a Thermal Bath. *Int. J. Syst. Evol. Microbiol.* **2017**, *67*, 1033–1038. [CrossRef]
19. Gorbatyuk, B.; Marczynski, G.T. Regulated Degradation of Chromosome Replication Proteins DnaA and CtrA in *Caulobacter crescentus*. *Mol. Microbiol.* **2005**, *55*, 1233–1245. [CrossRef]
20. Parte, A.C.; Carbasse, J.S.; Meier-Kolthoff, J.P.; Reimer, L.C.; Göker, M. List of Prokaryotic Names with Standing in Nomenclature (LPSN) Moves to the DSMZ. *Int. J. Syst. Evol. Microbiol.* **2020**, *70*, 5607–5612. [CrossRef]
21. Beilstein, F.; Dreiseikelmann, B. Bacteriophages of Freshwater *Brevundimonas vesicularis* Isolates. *Res. Microbiol.* **2006**, *157*, 213–219. [CrossRef]
22. West, D.; Lagenaur, C.; Agabian, N. Isolation and Characterization of *Caulobacter crecentus* Bacteriophage Phi Cd1. *J. Virol.* **1976**, *17*, 568–575. [CrossRef]

23. Ackermann, H.-W. Bacteriophage electron microscopy. In *Advances in Virus Research*; Elsevier Inc.: Amsterdam, The Netherlands, 2012; Volume 82, pp. 1–32. ISBN 978-0-12-394621-8.
24. Schmidt, J.M.; Stainer, R.Y. Isolation and Characterization of Bacteriophages Active against Stalked Bacteria. *J. Gen. Microbiol.* **1965**, *39*, 95–107. [CrossRef]
25. Kazaks, A.; Voronkova, T.; Rumnieks, J.; Dishlers, A.; Tars, K. Genome Structure of *Caulobacter* Phage PhiCb5. *J. Virol.* **2011**, *85*, 4628–4631. [CrossRef]
26. Friedrich, I.; Hollensteiner, J.; Schneider, D.; Poehlein, A.; Hertel, R.; Daniel, R. First Complete Genome Sequences of *Janthinobacterium lividum* EIF1 and EIF2 and Their Comparative Genome Analysis. *Genome Biol. Evol.* **2020**, *12*, 1782–1788. [CrossRef] [PubMed]
27. Friedrich, I.; Hollensteiner, J.; Scherf, J.; Weyergraf, J.; Klassen, A.; Poehlein, A.; Hertel, R.; Daniel, R. Complete Genome Sequence of *Stenotrophomonas indicatrix* DAIF1. *Microbiol. Resour. Announc.* **2021**, *10*, 15–17. [CrossRef]
28. Hollensteiner, J.; Friedrich, I.; Hollstein, L.; Lamping, J.; Wolf, K.; Liesegang, H.; Poehlein, A.; Hertel, R.; Daniel, R. Complete Genome Sequence of *Kinneretia* sp. Strain DAIF2, Isolated from a Freshwater Pond. *Microbiol. Resour. Announc.* **2021**, *10*, 5–7. [CrossRef]
29. Poindexter, J.S. Dimorphic prosthecate bacteria: The genera *Caulobacter*, *Asticcacaulis*, *Hyphomicrobium*, *Pedomicrobium*, *Hyphomonas* and *Thiodendron*. In *The Prokaryotes*; Springer: New York, NY, USA, 2006; Volume 5, pp. 72–90. ISBN 978-0-387-30745-9.
30. Klindworth, A.; Pruesse, E.; Schweer, T.; Peplies, J.; Quast, C.; Horn, M.; Glöckner, F.O. Evaluation of General 16S Ribosomal RNA Gene PCR Primers for Classical and Next-Generation Sequencing-Based Diversity Studies. *Nucleic Acids Res.* **2013**, *41*, e1. [CrossRef]
31. Fredriksson, N.J.; Hermansson, M.; Wilén, B.-M. The Choice of PCR Primers Has Great Impact on Assessments of Bacterial Community Diversity and Dynamics in a Wastewater Treatment Plant. *PLoS ONE* **2013**, *8*, e76431. [CrossRef]
32. Chen, S.; Zhou, Y.; Chen, Y.; Gu, J. Fastp: An Ultra-Fast All-in-One FASTQ Preprocessor. *Bioinformatics* **2018**, *34*, i884–i890. [CrossRef]
33. Zhang, J.; Kobert, K.; Flouri, T.; Stamatakis, A. PEAR: A Fast and Accurate Illumina Paired-End ReAd MergeR. *Bioinformatics* **2014**, *30*, 614–620. [CrossRef]
34. Martin, M. Cutadapt Removes Adapter Sequences from High-Throughput Sequencing Reads. *EMBnet J.* **2011**, *17*, 10–12. [CrossRef]
35. Rognes, T.; Flouri, T.; Nichols, B.; Quince, C.; Mahé, F. VSEARCH: A Versatile Open Source Tool for Metagenomics. *PeerJ* **2016**, *4*, e2584. [CrossRef]
36. Nearing, J.T.; Douglas, G.M.; Comeau, A.M.; Langille, M.G.I. Denoising the Denoisers: An Independent Evaluation of Microbiome Sequence Error-Correction Approaches. *PeerJ* **2018**, *2018*, e5364. [CrossRef]
37. Quast, C.; Pruesse, E.; Yilmaz, P.; Gerken, J.; Schweer, T.; Yarza, P.; Peplies, J.; Glöckner, F.O. The SILVA Ribosomal RNA Gene Database Project: Improved Data Processing and Web-Based Tools. *Nucleic Acids Res.* **2012**, *41*, D590–D596. [CrossRef]
38. Altschul, S.F.; Gish, W.; Miller, W.; Myers, E.W.; Lipman, D.J. Basic Local Alignment Search Tool. *J. Mol. Biol.* **1990**, *215*, 403–410. [CrossRef]
39. R Core Team. *R: A Language and Environment for Statistical Computing*; R Foundation for Statistical Computing: Vienna, Austria, 2020.
40. RStudio Team. *RStudio: Integrated Development for R*; RStudio, PBC: Boston, MA, USA, 2020.
41. Wickham, H. *Ggplot2—Elegant Graphics for Data Analysis*; Springer: New York, NY, USA, 2009; Volume 77, p. 3. ISBN 978-0-387-98140-6.
42. Bolger, A.M.; Lohse, M.; Usadel, B. Trimmomatic: A Flexible Trimmer for Illumina Sequence Data. *Bioinformatics* **2014**, *30*, 2114–2120. [CrossRef]
43. Magoč, T.; Salzberg, S.L. FLASH: Fast Length Adjustment of Short Reads to Improve Genome Assemblies. *Bioinformatics* **2011**, *27*, 2957–2963. [CrossRef]
44. Wick, R.R.; Judd, L.M.; Gorrie, C.L.; Holt, K.E. Unicycler: Resolving Bacterial Genome Assemblies from Short and Long Sequencing Reads. *PLoS Comput. Biol.* **2017**, *13*, e1005595. [CrossRef]
45. Bankevich, A.; Nurk, S.; Antipov, D.; Gurevich, A.A.; Dvorkin, M.; Kulikov, A.S.; Lesin, V.M.; Nikolenko, S.I.; Pham, S.; Prjibelski, A.D.; et al. SPAdes: A New Genome Assembly Algorithm and Its Applications to Single-Cell Sequencing. *J. Comput. Biol.* **2012**, *19*, 455–477. [CrossRef]
46. Vaser, R.; Sović, I.; Nagarajan, N.; Šikić, M. Fast and Accurate *de novo* Genome Assembly from Long Uncorrected Reads. *Genome Res.* **2017**, *27*, 737–746. [CrossRef]
47. BLAST Command Line Applications User Manual [Internet]. Available online: https://www.ncbi.nlm.nih.gov/books/NBK279690/ (accessed on 20 November 2020).
48. Langmead, B.; Salzberg, S.L. Fast Gapped-Read Alignment with Bowtie 2. *Nat. Methods* **2012**, *9*, 357–359. [CrossRef] [PubMed]
49. Li, H.; Handsaker, B.; Wysoker, A.; Fennell, T.; Ruan, J.; Homer, N.; Marth, G.; Abecasis, G.; Durbin, R. The Sequence Alignment/Map Format and SAMtools. *Bioinformatics* **2009**, *25*, 2078–2079. [CrossRef] [PubMed]
50. Arnold, K.; Gosling, J.; Holmes, D. *The Java Programming Language*, 4th ed.; Addison-Wesley Professional: Lebanon, IN, USA, 2005; ISBN 978-0-321-34980-4.

51. Walker, B.J.; Abeel, T.; Shea, T.; Priest, M.; Abouelliel, A.; Sakthikumar, S.; Cuomo, C.A.; Zeng, Q.; Wortman, J.; Young, S.K.; et al. Pilon: An Integrated Tool for Comprehensive Microbial Variant Detection and Genome Assembly Improvement. *PLoS ONE* **2014**, *9*, e112963. [CrossRef]
52. Okonechnikov, K.; Conesa, A.; García-Alcalde, F. Qualimap 2: Advanced Multi-Sample Quality Control for High-Throughput Sequencing Data. *Bioinformatics* **2016**, *32*, 292–294. [CrossRef]
53. Wick, R.R.; Schultz, M.B.; Zobel, J.; Holt, K.E. Bandage: Interactive Visualization of *de novo* Genome Assemblies. *Bioinformatics* **2015**, *31*, 3350–3352. [CrossRef] [PubMed]
54. Grissa, I.; Vergnaud, G.; Pourcel, C. CRISPRFinder: A Web Tool to Identify Clustered Regularly Interspaced Short Palindromic Repeats. *Nucleic Acids Res.* **2007**, *35*, W52–W57. [CrossRef] [PubMed]
55. Parks, D.H.; Imelfort, M.; Skennerton, C.T.; Hugenholtz, P.; Tyson, G.W. CheckM: Assessing the Quality of Microbial Genomes Recovered from Isolates, Single Cells, and Metagenomes. *Genome Res.* **2015**, *25*, 1043–1055. [CrossRef] [PubMed]
56. Tatusova, T.; DiCuccio, M.; Badretdin, A.; Chetvernin, V.; Nawrocki, E.P.; Zaslavsky, L.; Lomsadze, A.; Pruitt, K.D.; Borodovsky, M.; Ostell, J. NCBI Prokaryotic Genome Annotation Pipeline. *Nucleic Acids Res.* **2016**, *44*, 6614–6624. [CrossRef] [PubMed]
57. Otsuji, N.; Sekiguchi, M.; Iijima, T.; Takagi, Y. Induction of Phage Formation in the Lysogenic *Escherichia coli* K-12 by Mitomycin C. *Nature* **1959**, *184*, 1079–1080. [CrossRef]
58. Dietrich, S.; Wiegand, S.; Liesegang, H. TraV: A Genome Context Sensitive Transcriptome Browser. *PLoS ONE* **2014**, *9*, e93677. [CrossRef]
59. Hertel, R.; Volland, S.; Liesegang, H. Conjugative Reporter System for the Use in *Bacillus licheniformis* and Closely Related Bacilli. *Lett. Appl. Microbiol.* **2015**, *60*, 162–167. [CrossRef]
60. Chaumeil, P.-A.; Mussig, A.J.; Hugenholtz, P.; Parks, D.H. GTDB-Tk: A Toolkit to Classify Genomes with the Genome Taxonomy Database. *Bioinformatics* **2019**, *36*, 1925–1927. [CrossRef]
61. Pritchard, L.; Glover, R.H.; Humphris, S.; Elphinstone, J.G.; Toth, I.K. Genomics and Taxonomy in Diagnostics for Food Security: Soft-Rotting Enterobacterial Plant Pathogens. *Anal. Methods* **2016**, *8*, 12–24. [CrossRef]
62. Parks, D.H.; Chuvochina, M.; Chaumeil, P.A.; Rinke, C.; Mussig, A.J.; Hugenholtz, P. Selection of Representative Genomes for 24,706 Bacterial and Archaeal Species Clusters Provide a Complete Genome-Based Taxonomy. *BioRxiv* **2019**, 771964. [CrossRef]
63. Kanehisa, M.; Sato, Y.; Morishima, K. BlastKOALA and GhostKOALA: KEGG Tools for Functional Characterization of Genome and Metagenome Sequences. *J. Mol. Biol.* **2016**, *428*, 726–731. [CrossRef] [PubMed]
64. Medema, M.H.; Blin, K.; Cimermancic, P.; de Jager, V.; Zakrzewski, P.; Fischbach, M.A.; Weber, T.; Takano, E.; Breitling, R. AntiSMASH: Rapid Identification, Annotation and Analysis of Secondary Metabolite Biosynthesis Gene Clusters in Bacterial and Fungal Genome Sequences. *Nucleic Acids Res.* **2011**, *39*, W339–W346. [CrossRef]
65. Blin, K.; Shaw, S.; Steinke, K.; Villebro, R.; Ziemert, N.; Lee, S.Y.; Medema, M.H.; Weber, T. AntiSMASH 5.0: Updates to the Secondary Metabolite Genome Mining Pipeline. *Nucleic Acids Res.* **2019**, *47*, W81–W87. [CrossRef]
66. Arndt, D.; Grant, J.R.; Marcu, A.; Sajed, T.; Pon, A.; Liang, Y.; Wishart, D.S. PHASTER: A Better, Faster Version of the PHAST Phage Search Tool. *Nucleic Acids Res.* **2016**, *44*, W16–W21. [CrossRef] [PubMed]
67. Gibson, M.K.; Forsberg, K.J.; Dantas, G. Improved Annotation of Antibiotic Resistance Determinants Reveals Microbial Resistomes Cluster by Ecology. *ISME J.* **2015**, *9*, 207–216. [CrossRef] [PubMed]
68. Claus, D. A Standardized Gram Staining Procedure. *World J. Microbiol. Biotechnol.* **1992**, *8*, 451–452. [CrossRef]
69. Bruder, S.; Reifenrath, M.; Thomik, T.; Boles, E.; Herzog, K. Parallelied Online Biomass Monitoring in Shake Flasks Enables Efficient Strain and Carbon Source Dependent Growth Characterisation of *Saccharomyces cerevisiae*. *Microb. Cell Fact.* **2016**, *15*, 127. [CrossRef]
70. Macy, J.M.; Snellen, J.E.; Hungate, R.E. Use of Syringe Methods for Anaerobiosis. *Am. J. Clin. Nutr.* **1972**, *25*, 1318–1323. [CrossRef]
71. Clarke, P.H.; Cowan, S.T. Biochemical Methods for Bacteriology. *J. Gen. Microbiol.* **1952**, *6*, 187–197. [CrossRef]
72. Meier-Kolthoff, J.P.; Göker, M. TYGS Is an Automated High-Throughput Platform for State-of-the-Art Genome-Based Taxonomy. *Nat. Commun.* **2019**, *10*, 2182. [CrossRef] [PubMed]
73. Richter, M.; Rosselló-Móra, R. Shifting the Genomic Gold Standard for the Prokaryotic Species Definition. *Proc. Natl. Acad. Sci. USA* **2009**, *106*, 19126–19131. [CrossRef]
74. Reimer, L.C.; Vetcininova, A.; Carbasse, J.S.; Söhngen, C.; Gleim, D.; Ebeling, C.; Overmann, J. BacDive in 2019: Bacterial Phenotypic Data for High-Throughput Biodiversity Analysis. *Nucleic Acids Res.* **2019**, *47*, D631–D636. [CrossRef]
75. Milke, J.; Gałczyńska, M.; Wróbel, J. The Importance of Biological and Ecological Properties of *Phragmites australis* (Cav.) Trin. Ex Steud., in Phytoremendiation of Aquatic Ecosystems—The Review. *Water* **2020**, *12*, 1770. [CrossRef]
76. Fazi, S.; Amalfitano, S.; Piccini, C.; Zoppini, A.; Puddu, A.; Pernthaler, J. Colonization of Overlaying Water by Bacteria from Dry River Sediments. *Environ. Microbiol.* **2008**, *10*, 2760–2772. [CrossRef]
77. Eberspächer, J.; Lingens, F. The genus *Phenylobacterium*. In *The Prokaryotes*; Springer: New York, NY, USA, 2006; pp. 250–256. ISBN 978-0-387-30745-9.
78. Vancanneyt, M.; Segers, P.; Abraham, W.; Vos, P.D. *Brevundimonas*. In *Bergey's Manual of Systematics of Archaea and Bacteria*; Trujillo, M.E., Dedysh, S., DeVos, P., Hedlund, B., Kämpfer, P., Rainey, F.A., Whitman, W.B., Eds.; John Wiley & Sons, Inc.: Hoboken, NJ, USA, 2015; pp. 1–14. ISBN 978-1-118-96060-8.

79. Willms, I.M.; Yuan, J.; Penone, C.; Goldmann, K.; Vogt, J.; Wubet, T.; Schöning, I.; Schrumpf, M.; Buscot, F.; Nacke, H. Distribution of Medically Relevant Antibiotic Resistance Genes and Mobile Genetic Elements in Soils of Temperate Forests and Grasslands Varying in Land Use. *Genes* **2020**, *11*, 150. [CrossRef] [PubMed]
80. Zhang, Z.; Du, C.; de Barsy, F.; Liem, M.; Liakopoulos, A.; van Wezel, G.P.; Choi, Y.H.; Claessen, D.; Rozen, D.E. Antibiotic Production in *Streptomyces* Is Organized by a Division of Labor through Terminal Genomic Differentiation. *Sci. Adv.* **2020**, *6*, eaay5781. [CrossRef]
81. Tomasch, J.; Wang, H.; Hall, A.T.K.; Patzelt, D.; Preusse, M.; Petersen, J.; Brinkmann, H.; Bunk, B.; Bhuju, S.; Jarek, M.; et al. Packaging of *Dinoroseobacter shibae* DNA into Gene Transfer Agent Particles Is Not Random. *Genome Biol. Evol.* **2018**, *10*, 359–369. [CrossRef] [PubMed]
82. McLaughlin, J.R.; Wong, H.C.; Ting, Y.E.; Van Arsdell, J.N.; Chang, S. Control of Lysogeny and Immunity of *Bacillus subtilis* Temperate Bacteriophage SP Beta by Its d Gene. *J. Bacteriol.* **1986**, *167*, 952–959. [CrossRef] [PubMed]
83. Rettenmier, C.W.; Gingell, B.; Hemphill, H.E. The Role of Temperate Bacteriophage SP Beta in Prophage-Mediated Interference in *Bacillus subtilis*. *Can. J. Microbiol.* **1979**, *25*, 1345–1351. [CrossRef] [PubMed]
84. Yamamoto, T.; Obana, N.; Yee, L.M.; Asai, K.; Nomura, N.; Nakamura, K. SP10 Infectivity Is Aborted after Bacteriophage SP10 Infection Induces NonA Transcription on the Prophage SPβ Region of the *Bacillus subtilis* Genome. *J. Bacteriol.* **2014**, *196*, 693–706. [CrossRef]